THE JOURNAL OF BIOLOGICAL CHEMISTRY VOL. 281, NO. 47, pp. 36466–36476, November 24, 2006

Spontaneous Formation of L-Isoaspartate and Gain of Function in Fibronectin*

Received for publication, May 18, 2006, and in revised form, September 15, 2006 Published, JBC Papers in Press, October 2, 2006, DOI 10.1074/jbc.M604812200

Flavio Curnis[‡], Renato Longhi[§], Luca Crippa[‡], Angela Cattaneo[‡], Eleonora Dondossola[‡], Angela Bachi[‡], and Angelo Corti[‡1]

From the [‡]Department of Oncology, Cancer Immunotherapy and Gene Therapy Program and Italian Institute of Technology Network Research Unit of Molecular Neuroscience, San Raffaele Scientific Institute, Via Olgettina 58, 20132 Milan, and [§]Istituto di Chimica del Riconoscimento Molecolare, Consiglio Nazionale delle Ricerche, Via M. Bianco 9, 20131 Milan, Italy

Isoaspartate formation in extracellular matrix proteins, by aspartate isomerization or asparagine deamidation, is generally viewed as a degradation reaction occurring *in vivo* during tissue aging. For instance, non-enzymatic isoaspartate formation at RGD-integrin binding sites causes loss of cell adhesion sites, which in turn can be enzymatically "repaired" to RGD by protein-L-*iso*Asp-*O*-methyltransferase. We show here that isoaspartate formation is also a mechanism for extracellular matrix activation. In particular, we show that deamidation of Asn[263] at the Asn-Gly-Arg (NGR) site in fibronectin N-terminal region generates an $\alpha_v\beta_3$-integrin binding site containing the L-*iso*DGR sequence, which is enzymatically "deactivated" to DGR by protein-L-*iso*Asp-*O*-methyltransferase. Furthermore, rapid NGR-to-*iso*DGR sequence transition in fibronectin fragments generates $\alpha_v\beta_3$ antagonists (named "isonectins") that competitively bind RGD binding sites and inhibit endothelial cell adhesion, proliferation, and tumor growth. Time-dependent generation of *iso*DGR may represent a sort of molecular clock for activating latent integrin binding sites in proteins.

Fibronectins are adhesive proteins that mediate a variety of cellular interactions with extracellular matrix and play important roles in hemostasis, thrombosis, inflammation, wound repair, angiogenesis, and embryogenesis (1, 2). About 20 isoforms of human fibronectin can be generated as a result of alternative splicing of the primary transcript (1, 3). Fibronectins are large glycoproteins (~450 kDa) composed of two nearly identical disulfide-bonded subunits present in most body fluids and extracellular matrix of many tissues. Each subunit consists of three types of repeating homologous modules termed FN-I, FN-II, and FN-III repeats. Alternatively spliced modules, called EDA, EDB, and IIICS, can also be present (1, 3). Single modules or groups of modules may contain binding sites for different molecules, including sulfated glycosaminoglycans, DNA, gelatin, heparin, and fibrin (1, 3, 4). Furthermore, fibronectins contain binding sites for about half of the known cell surface integrin receptors (5, 6). In particular, the FN-III_{10} repeat contains an RGD site that can bind $\alpha_3\beta_1$, $\alpha_5\beta_1$, $\alpha_v\beta_1$, $\alpha_v\beta_3$, $\alpha_v\beta_5$, $\alpha_v\beta_6$, $\alpha_8\beta_1$, and $\alpha II_b\beta_3$ integrins, while the FN-III_9 repeat contains the so-called "synergy site" PHSRN that cooperates with RGD in the binding of $\alpha_5\beta_1$ and $\alpha II_b\beta_3$ (1, 7).

Primary and tertiary structure analysis of human fibronectin showed that this protein contains two GNGRG loops, located in FN-I_5 and FN-I_7 modules, that are conserved in bovine, murine, rat, amphibian, and fish (8). Two additional NGR sites, less conserved, are also present in human FN-II_1 and FN-III_9 (see Fig. 1). Recent experimental work showed that peptides containing the NGR motif can inhibit $\alpha_5\beta_1$- and $\alpha_v\beta_1$-mediated cell adhesion to fibronectin (9).

These notions prompted us to investigate the functional role of NGR in fibronectin. We observed that the NGR sequence of FN-I_5 (residues 263–265) promotes endothelial cell adhesion via an unusual mechanism based on non-enzymatic deamidation of Asn[263] to L-*iso*Asp, generating *iso*DGR, a new cell adhesion motif. Furthermore, we show that $\alpha_v\beta_3$ integrin is an important receptor of *iso*DGR and that the deamidated FN-I_5 module (named "isonectin-1") regulates endothelial cell adhesion and inhibits tumor growth. Finally, we show that this motif is regulated in a negative manner by protein-L-*iso*Asp-*O*-methyltransferase (PIMT).[2] Based on these findings we propose a new "activation/deactivation" model for *iso*Asp "formation/removal" in fibronectin.

EXPERIMENTAL PROCEDURES

Cell Lines and Reagents—Mouse RMA lymphoma cells, B16 melanoma, and EA.hy926 cells (human endothelial cells fused with human lung carcinoma A549 cells) were cultured as described previously (10, 11). Human microvasculature endothelial cells, HMEC-1, were provided by Dr. A. Manfredi (San Raffaele H Scientific Institute, Milan, Italy) and cultured in MCDB131 medium supplemented with 2 mM L-glutamine, 10 units/ml penicillin, 10 units/ml streptomycin, 25 ng/ml amphotericin B, 10% fetal bovine serum, 10 ng/ml human recombi-

* This work was supported in part by Associazione Italiana per la Ricerca sul Cancro. The costs of publication of this article were defrayed in part by the payment of page charges. This article must therefore be hereby marked "*advertisement*" in accordance with 18 U.S.C. Section 1734 solely to indicate this fact.

[1] To whom correspondence should be addressed. Tel.: 39-02-26434802; Fax: 39-02-26434786; E-mail: corti.angelo@hsr.it.

[2] The abbreviations used are: PIMT protein-L-*iso*Asp/D-Asp-*O*-methyltransferase; TNFα, tumor necrosis factor α; MALDI-TOF, matrix-assisted laser desorption ionization time-of-flight; BSA, bovine serum albumin; DMEM, Dulbecco's modified Eagle's medium; ECM, extracellular matrix; ELISA, enzyme-linked immunosorbent assay; RP-HPLC, reverse phase high performance liquid chromatography; HMEC, human microvasculature endothelial cell.

nant epidermal growth factor (R&D Systems, Inc.), and 1 μg/ml hydrocortisone (complete medium). Crystal violet (Fluka Chemie), bovine serum albumin (BSA), goat anti-rabbit IgG horseradish peroxidase conjugate, FN-70 kDa, FN-45 kDa, and FN-30 kDa fragments (Sigma), RetroNectin (Takara Biomedicals), human $\alpha_v\beta_3$, $\alpha_5\beta_1$, and $\alpha_1\beta_1$ integrins (Immunological Sciences), and streptavidin peroxidase (Società Prodotti Antibiotici) were used. Human fibronectin was freshly isolated from plasma by affinity chromatography on gelatin-Sepharose as described (12).

Preparation and Characterization of Recombinant FN-I_{4-5} and FN-I_{4-5}SGS—The cDNA coding for human fibronectin fourth-fifth type I repeats (FN-I_{4-5}; residues 184–273 of fibronectin) was prepared by reverse transcriptase PCR on MSR-3-mel cells total RNA (13) using the following primers: 5′-CTGGATCCGAGAAGTGTTTTGATCATGCTGCTGGG (forward) and 5′-TATATTAAGCTTTCAGTGCCTCTCACACTTCC (reverse). A control fragment with NGR replaced with SGS (FN-I_{4-5}SGS), was generated by PCR on FN-I_{4-5} plasmid using the above forward primer and the following reverse primer, 5′-TATATTAAGCTTTCAGTGCCTCTCACACTTCCACTCTCCACTGCCGCTG. Amplified fragments were cloned into a pRSET-A plasmid (Invitrogen), expressed in BL21(DE3)pLysS *Escherichia coli* cells as soluble proteins (with a His tag at the N terminus), and purified from cell extracts by metal-chelate affinity chromatography.

Preparation and Characterization of Synthetic Peptides—Various peptides (biotinylated and non-biotinylated) were prepared by chemical synthesis using an Applied Biosystem model 433A peptide synthesizer. Amino acids in L-configuration were used except when indicated. A synthetic peptide corresponding to the fifth type I repeat of human fibronectin (FN-I_5), residues 230–274 of mature protein (Swiss-Prot accession number P02751), was also synthesized with an additional N-terminal acetyl-glycine and with Glu^{250} in place of Asp^{250}. To promote disulfide formation between Cys^{258}-Cys^{270} and Cys^{231}-Cys^{260} in FN-I_5 (see Fig. 1), Cys^{258} and Cys^{270} were protected with S-trityl groups (removable by trifluoroacetic acid after side-chain deprotection and cleavage from the resin), whereas Cys^{231} and Cys^{260} were protected with S-acetamidomethyl groups (removable by treatment with iodine). After RP-HPLC purification of peptide, the Cys^{258}-Cys^{270} disulfide bridge was formed by incubating 20 μmol of peptide in 300 ml of 8% Me_2SO at pH 7 (room temperature, overnight). The peptide was then purified by RP-HPLC and lyophilized. To form the second Cys^{231}-Cys^{260} disulfide bridge, 13.5 μmol of peptide was dissolved in 67 ml of 80% v/v acetic acid and mixed with 0.135 ml of 1 N hydrochloric acid. Then, 21 mg of iodine, dissolved in 2 ml of methanol, was added to the peptide solution under stirring. After 90 min, 1 mmol of ascorbic acid was added to quench iodine. The peptide was then purified by RP-HPLC. All peptides were dissolved in sterile water and stored in aliquots at −20 °C. Peptide purity was analyzed by RP-HPLC. Free sulfhydryl groups in all peptide preparations were <0.1% as checked by titration with Ellman's reagent (Pierce). Peptide identity was checked by MALDI-TOF or electrospray ionization mass spectrometry. The molecular mass of peptides used throughout this work was similar to the expected value. Electrospray ionization mass spectrometry analysis of FN-I_5 showed the presence of an additional component of +144 Da, corresponding to FN-I_5 with unremoved acetamidomethyl groups.

Preparation and Characterization of CNGRC-TNF, CDGRC-TNF, ACDCRGDCFC-TNF, and CNGRC-TNF_{1-11} Conjugates—Murine TNF, CNGRC-TNF (consisting of murine TNF fused with the C terminus of CNGRCG), and ACDCRGDCFC-TNF conjugates were prepared by recombinant DNA technology as described (14, 15). The cDNA coding for CDGRC-TNF (murine TNF fused with the C terminus of CDGRCG) was prepared by PCR on CNGRC-TNF plasmid (14) using the primers 5′-CACCATGGGCAACGGCCGTGGCGGCGTC (forward) and 5′-TCAGGATCCTCACAGGGCAATGATCCCAAAGTAGAC (reverse). The amplified cDNA was cloned into the pET101/D-TOPO plasmid (Invitrogen), expressed in BL21(DE3) *E. coli* cells (Novagen), and purified from cell extracts by affinity chromatography on soluble p75-TNF receptor-Sepharose essentially as described previously for CNGRC-TNF (16). Both CNGRC-TNF and CDGRC-TNF were subjected to a refolding procedure as described previously (14). Protein purity and identity were checked by SDS-PAGE, electrospray mass spectrometry, and gel filtration chromatography. The *in vitro* cytolytic activity of CNGRC-TNF and CDGRC-TNF, measured by standard cytolytic assay with L-M mouse fibroblasts (17), were 2.96 (± 0.56) × 10^8 and 2.59 (± 0.69) × 10^8 units/mg, respectively. CNGRC-TNF_{1-11}, corresponding to the N-terminal sequence of NGR-TNF (lacking TNF activity) and CARAC-TNF_{1-11} peptide, were prepared by chemical synthesis as described above.

Accelerated Aging (Heat Treatment) of Fibronectin Fragments and Peptides—Fibronectin fragments, peptides, and peptide-TNF conjugates were diluted in 0.1 M ammonium bicarbonate buffer, pH 8.5, incubated for 16 h at 37 °C, and stored at −20 °C until analysis. These products are hereinafter referred to as "heat treated."

Isoaspartate (isoAsp) Quantification—*iso*Asp content in proteins and peptides was quantified using the IsoQuant isoaspartate detection kit (Promega). The *iso*Asp content in fibronectin (freshly isolated from human plasma) and FN-30 kDa fragment was 0.048 and 0.026 pmol/pmol of protein, respectively.

Cell Adhesion Assay and PIMT Treatment—Untreated and heat-treated fibronectin fragments, peptides, and peptide-TNF conjugates were diluted at the desired concentration with 150 mM sodium chloride, 50 mM sodium phosphate, pH 7.3, and added to 96-well polyvinyl chloride microtiter plates (Falcon; BD Biosciences). After overnight incubation at 4 °C, the plates were washed, seeded with EA.hy926 cells in DMEM containing 0.1% BSA (40,000 cells/well), and left to incubate for 2–3 h at 37 °C, 5% CO_2. Adherent cells were fixed and stained with crystal violet as described (11). The effect of PIMT on the pro-adhesive properties of different fragments was investigated as follows. Microtiter plates were coated with various products as described above and washed with 0.9% sodium chloride. Each well was then filled with 45 μl of a solution containing 0.02 mM *S*-adenosyl-L-methionine in 150 mM sodium chloride, 50 mM sodium phosphate buffer, pH 6.8, and 5 μl of PIMT solution (from the IsoQuant isoaspartate detection kit; Promega) (final volume 50 μl/well) and incubated at 37 °C for 16 h. After incu-

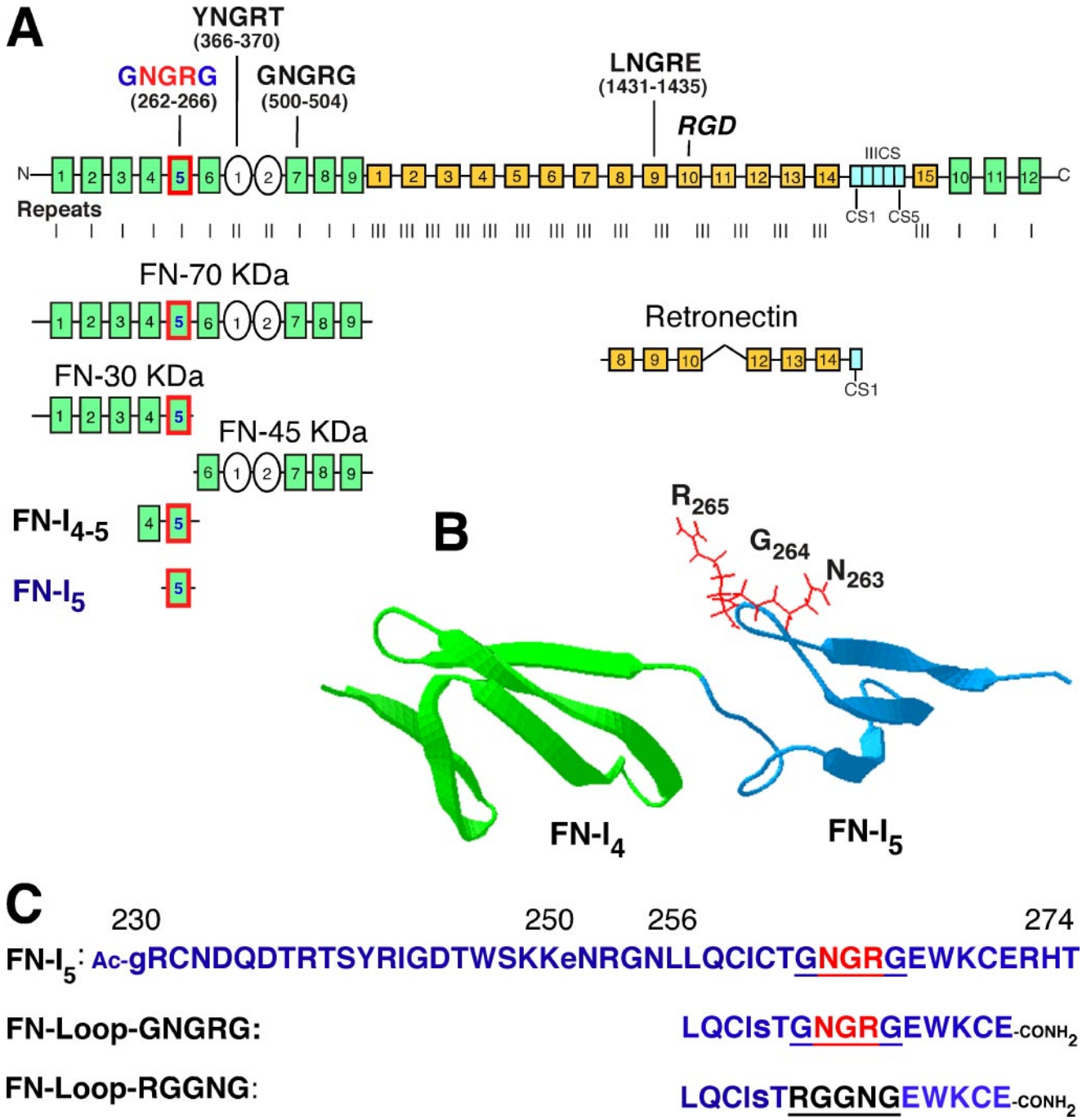

FIGURE 1. **Schematic representation, three-dimensional structure, and primary sequence of fibronectin fragments.** *A*, type I repeats (*rectangles*), type II repeats (*ovals*), type III repeats (*squares*). Modules containing NGR and RGD sequences are indicated. Natural fragments (*FN-70*, *FN-45*, and *FN-30 kDa*), retronectin, FN-I_{4-5}, and FN-I_5 are represented. *B*, three-dimensional PDB structure of FN-I_{4-5} (Protein Data Bank code 1FBR). The side chains of the NGR motif (Asn^{263}, Gly^{264}, and Arg^{265}) are shown. *C*, primary sequence of synthetic FN-I_5, FN-Loop-GNGRG, and FN-Loop-RGGNG peptides.

bation the plates were washed with 0.9% sodium chloride, and cell adhesion assay was performed as described above.

Binding of Peptides and Proteins to Integrins—Human $\alpha_v\beta_3$, $\alpha_5\beta_1$, and $\alpha_1\beta_1$ integrin solutions, 0.5–2 μg/ml in phosphate-buffered saline with Ca^{2+} and Mg^{2+} (DPBS; Cambrex), were added to 96-well polyvinylchloride microtiter plates (50 μl/well) and left to incubate overnight at 4 °C. All subsequent steps were carried out at room temperature. The plates were washed with DPBS and further incubated with DPBS containing 3% BSA (200 μl/well, 1 h). The plates were washed and filled with CNGRC-TNF or TNF solutions (5 μg/ml, 50 μl/well in 3% BSA-DPBS) and left to incubate for 2 h. After washing with DPBS, each well was incubated with purified rabbit anti-murine TNF IgGs in 3% BSA-DPBS containing 1% normal goat serum (10 μg/ml, 50 μl/well, 1 h) followed by a goat anti-rabbit peroxidase conjugate in the same buffer (50 μl/well, 1 h). Bound peroxidase was detected by adding o-phenylendiamine chromogenic substrate. Binding of biotinylated peptides (CNGRC-TNF_{1-11}, CARAC-TNF_{1-11}, and FN-I_5) to purified integrins was studied using streptavidin peroxidase conjugate com-

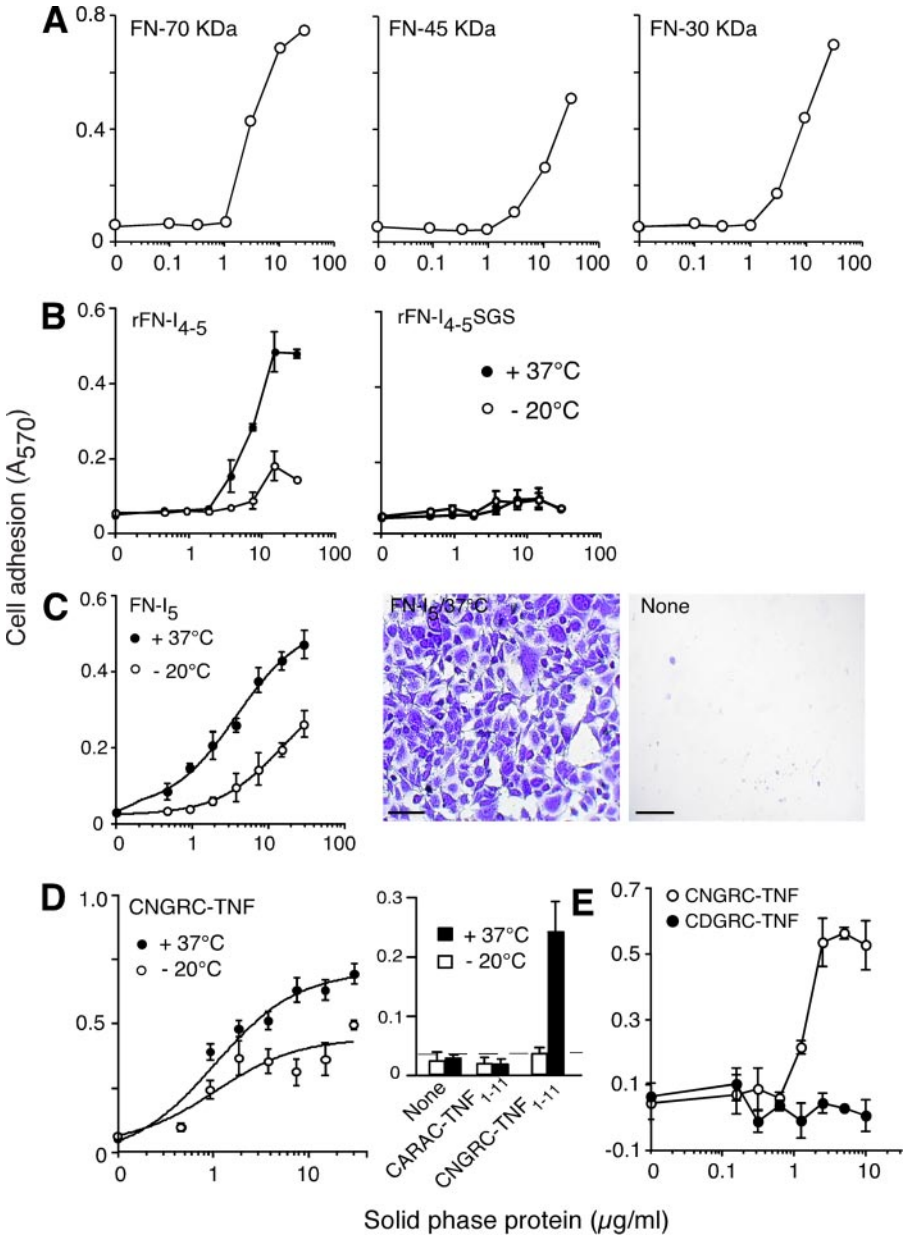

FIGURE 2. **Accelerated aging of fibronectin fragments increases their pro-adhesive properties.** Adhesion of endothelial EA.hy926 cells to microtiter plates coated with various peptides and proteins before (−20 °C) and after (+37 °C) accelerated aging. *A*, adhesion to natural proteolytic fragments FN-70 kDa, FN-45 kDa, and FN-30 kDa. *B*, recombinant FN-I_{4-5} or control FN-I_{4-5}SGS fragment. *C*, synthetic FN-I_5. *D*, recombinant CNGRC-TNF, CNGRC-TNF_{1-11}, and control CARAC-TNF_{1-11} peptide; *E*, CDGRC-TNF. Microphotograph of wells coated with 30 μg/ml of heat-treated FN-I_5 or BSA (*C*, *right*), ×200; *bar* indicates 50-μm scale. Cell adhesion assays were carried out as described under "Experimental Procedures." Mean ± S.E. ($n = 2$).

plexes. Complexes were prepared by mixing various quantities (0.5–1 μg) of heat-treated biotinylated peptides in DPBS containing 3% BSA with 0.03 units of streptavidin peroxidase (binding capacity 1 μg of biotin/unit of streptavidin peroxidase) (final volume 15 μl). Complexes were diluted in 3% BSA-DPBS (1:500), added to microtiter plates coated with integrins as described above, and incubated for 2 h at room temperature. After washing with DPBS, bound peroxidase was detected by chromogenic reaction as described above. Each assay was carried out in triplicate.

Inhibition of Endothelial Cell Proliferation—HMEC-1 cells (8×10^3) in complete medium were seeded in 96-well plate (100 μl/well). After 2 h of incubation at 37 °C, 5% CO_2, 100 μl of peptide solution in complete medium (100 μM) was added to each well. Cells were further incubated for 72 h at 37 °C, 5% CO_2. The number of viable cells present within each well was then determined by 3-(4,5-dimethylthiazol-2-yl)-2,5-diphenyltetrazolium bromide assay using a calibration curve generated by plating different amounts of cells.

In Vivo Studies—Studies on animal models were approved by the Ethical Committee of the San Raffaele H Scientific Institute and performed according to the prescribed guidelines. C57BL/6N mice (Charles River Laboratories, Calco, Italy) weighing 16–18 g were challenged with subcutaneous injection in the left flank of 7×10^4 RMA living cells; 4 days later, mice were treated daily with 200 μg of heat-treated FN-I_5 (100 μl) in 0.9% sodium chloride (intraperitoneal). Tumor growth was monitored by measuring tumors with calipers as previously described (18). Animals were sacrificed before tumors reached 1.0–1.3 cm in diameter. Tumor sizes are shown as mean ± S.E. (five animals/group).

RESULTS

Accelerated Aging of Fibronectin Fragments Generates NGR-dependent Adhesion Sites—The adhesion of EA.hy926 cells to natural, recombinant, and synthetic fibronectin fragments containing the NGR motif was studied. First, the following proteolytic fragments of fibronectin were studied: (*a*) FN-70 kDa, containing the FN-I_{1-9} and FN-II_{1-2} repeats; (*b*) FN-30 kDa, containing the FN-I_{1-5} repeats; and (*c*) FN-45 kDa, containing the FN-I_{6-9} and FN-II_{1-2} repeats (see Fig. 1 for a schematic representation). All fragments, after adsorption to microtiter plates, induced cell adhesion and spreading (Fig. 2*A*), suggesting the presence of pro-adhesive sites in these regions.

To investigate the role of the NGR motif in this phenomenon we analyzed the pro-adhesive properties of FN-I_{4-5} and FN-I_{4-5}SGS fragments, the latter corresponding to a mutant with SGS in place of NGR (residues 263–265). Recombinant FN-I_{4-5}, but not the SGS mutant, promoted cell adhesion (Fig. 2*B*). When we incubated these fragments in 0.1 M ammonium bicarbonate buffer, pH 8.5, for 16 h at 37 °C (from now on this

treatment will be called "heat treatment"), we observed an increase of cell adhesion to FN-I_{4-5}, but not to FN-I_{4-5}SGS (Fig. 2*B*). This suggests that a cell adhesion site, somehow related to the NGR sequence, was generated by accelerated aging. Similar results were obtained with synthetic FN-I_5 (Fig. 2*C*).

To assess whether the NGR motif was sufficient for mediating this phenomenon, we investigated the pro-adhesive properties of short peptides containing the NGR motif before and after heat treatment. Because the NGR tripeptide is unlikely to fold and to bind to microtiter plates, we introduced two flanking cysteines. The rationale for using flanking cysteines was based on the fact that the predicted conformation of CNGRC peptide, by molecular dynamic simulation, is similar to that of the GNGRG loop of FN-I_5 repeat (8). Furthermore, we fused this peptide to TNF (CNGRC-TNF) or to the first eleven residues of TNF (CNGRC-TNF_{1-11}, devoid of TNF activity) to enable adsorption to microtiter plates. As expected, heat treatment of CNGRC-TNF increased cell adhesion (Fig. 2*D*). No adhesion was observed to TNF alone either before or after heat treatment (data not shown). Similarly, heat treatment of CNGRC-TNF_{1-11}, but not of CARAC-TNF_{1-11} (a control peptide), increased cell adhesion (Fig. 2*D*, *right*).

These results support the hypothesis that the NGR motif is sufficient for promoting cell adhesion after heat treatment. Interestingly, a CDGRC-TNF conjugate, prepared by recombinant DNA technology, was completely inactive (Fig. 2*E*), suggesting that Asn is a crucial residue for the enhanced activity. In conclusion, these results suggest that structural changes related to the Asn residue of NGR motif in FN-I_5 lead to generation of a pro-adhesive site.

Deamidation of the NGR Motif Is Associated with Increased Cell Adhesion—It is well known that the Asn residues, particularly when followed by Gly, can undergo non-enzymatic deamidation via succinimide intermediate at physiological pH (19–23). This reaction leads to formation of Asp and *iso*Asp, predominantly in L-configuration (24). Accordingly, heat treatment of FN-I_5, CNGRC-TNF, and CNGRC peptides increased their molecular mass by ~1 Da as measured by mass spectrometry analysis (data not shown). Furthermore, >0.5 mol *iso*Asp/mol of heat-treated CNGRC-TNF subunit was detected using the IsoQuant kit.

To assess whether the enhanced adhesive properties of FN-I_5 after heat treatment depended on NGR deamidation, we incubated the heat-treated FN-I_5 and CNGRC-TNF with PIMT, an enzyme that converts L-*iso*Asp and D-Asp residues to L-Asp (25–29). PIMT almost completely inhibited the pro-adhesive activity of heat-treated FN-I_5 and CNGRC-TNF (Fig. 3*A*). Moreover, this enzymatic treatment partially inhibited the pro-adhesive properties of natural FN-30 kDa (Fig. 3*B*) and FN-45 kDa fragments (data not shown), suggesting that Asn deamidation can occur also in natural fibronectin fragments. To assess the specificity of this reaction we evaluated the effect of PIMT on retronectin, an FN fragment that is known to promote cell adhesion via RGD (see Fig. 1). As expected, in this case no inhibition was observed after enzymatic treatment (Fig. 3*B*). Conversely, in this case we observed a modest but significant increase. This was not totally unexpected as also RGD can

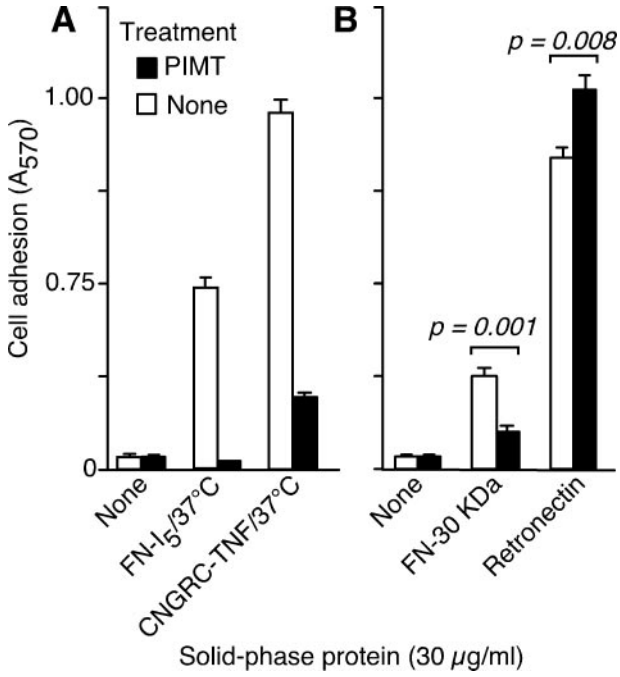

FIGURE 3. **The pro-adhesive properties of fibronectin fragments containing NGR are inhibited by PIMT.** Microtiter plates were coated with heat-treated FN-I_5 or CNGRC-TNF (*A*) or with natural FN-30 kDa or retronectin (*B*). Adsorbed proteins were then treated with PIMT for 16 h at 37 °C. After incubation the enzyme solution was removed, and EA.hy926 cell adhesion assay was performed as described under "Experimental Procedures." Mean ± S.E. ($n = 4$).

undergo isomerization of Asp residues, with formation of *iso*Asp and loss of function (20, 24, 30, 31). Thus, in this case PIMT is expected to "repair" RGD and increase cell adhesion. In conclusion, these results suggest that NGR deamidation, in contrast to RGD isomerization, is associated with a "gain of function" in cell adhesion assays.

Mechanism of NGR Deamidation—The mechanism and the kinetics of peptide deamidation in DMEM, pH 7.53, and in 0.1 M ammonium bicarbonate, pH 8.5, were then investigated. To this aim the CNGRCGVRY peptide (called NGR-2C) was synthesized and analyzed by reverse-phase HPLC before and after incubation at 37 °C. Residues GVRY were added to the C terminus of CNGRC to enable detection and column adsorption. In addition, two peptides called CDGRCGVRY (DGR-2C) and CisoDGRCGVRY (isoDGR-2C) corresponding to the same sequence of NGR-2C except for the presence of L-Asp and L-*iso*Asp in place of L-Asn, respectively, were prepared and analyzed by HPLC. The half-life of NGR-2C at pH 7.53 and pH 8.5, estimated from the height of the main chromatographic peak (Fig. 4*A*, *peak 1*), was ~4 and 2 h, respectively (Fig. 4*A*, *inset*). In contrast, DGR-2C and *iso*DGR-2C under the same conditions were considerably more stable than NGR-2C (not shown).

Further studies on NGR-2C stability in 150 mM sodium chloride, 25 mM Hepes, pH 7.4, and in 150 mM sodium chloride, 50 mM sodium phosphate, pH 7.3, showed that 1 and 5% of peptide, respectively, was degraded after 1 day at 4 °C. These values increased to 27 and 86%, respectively, after 1 day at 37 °C. Of note, the peptide was stable for more than 1 week at 4 and 37 °C when stored in water (pH 5.6). Thus, the degradation reaction strongly depends on buffer composition.

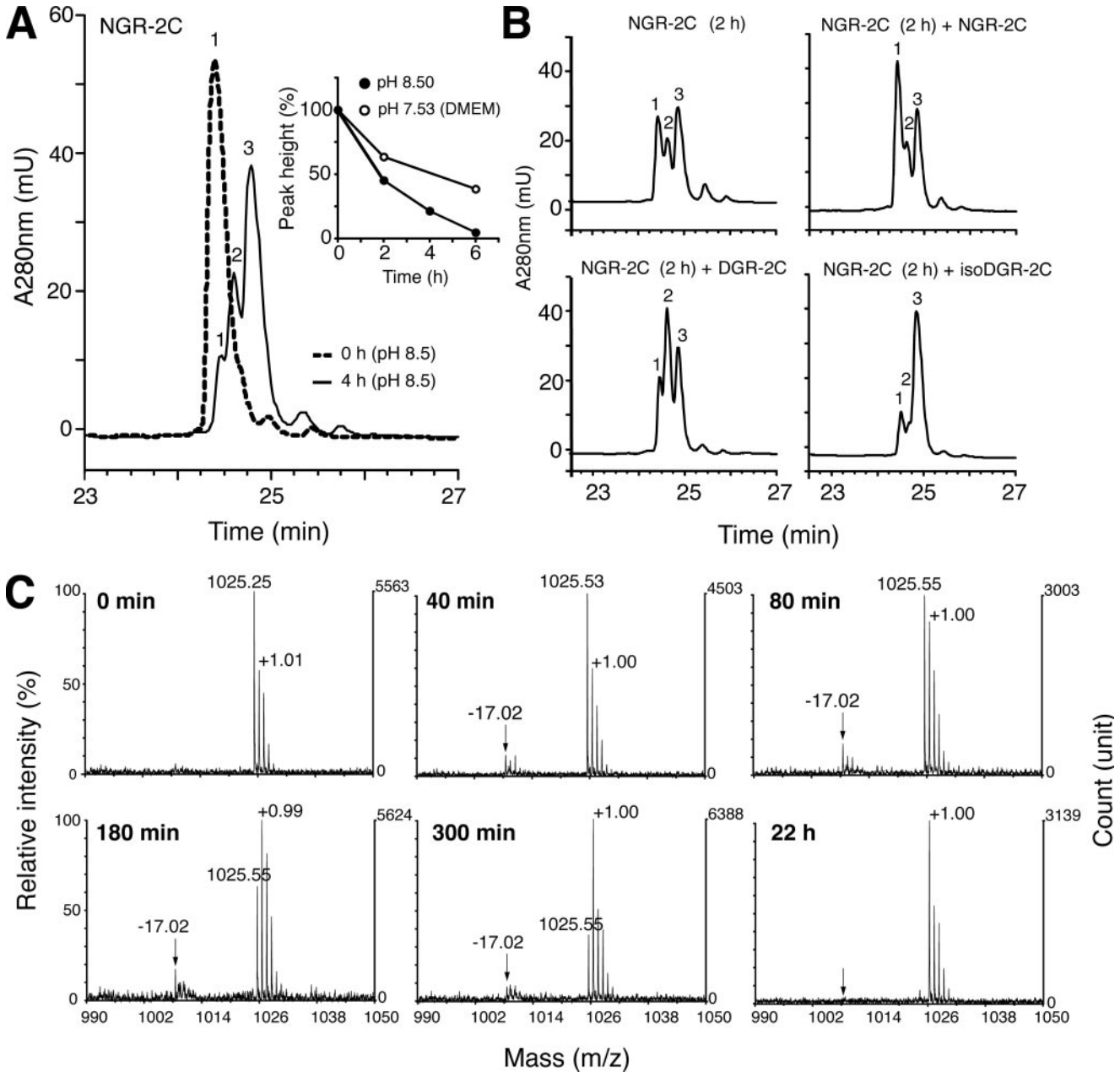

FIGURE 4. **Peptides containing NGR are unstable and rapidly convert to compounds corresponding to DGR, *iso*DGR, and succinimide intermediate.** *A*, RP-HPLC analysis of CNGRCGVRY (*NGR-2C*) before and after incubation for 4 h at 37 °C in 0.1 M ammonium bicarbonate buffer, pH 8.5, or in DMEM, pH 7.53. RP-HPLC was performed on a C-18 column (PepMap C18; PerSeptive Biosystem) as follows: buffer A, 0.1% trifluoroacetic acid in water; buffer B, 95% acetonitrile, 0.1% trifluoroacetic acid; 0% B for 10 min, linear gradient 20–40% B in 30 min, 100% B for 10 min; 0% B for 15 min (flow rate, 0.5 ml/min). *B*, peaks 1, 2, and 3 identification by NGR-2C spiking with equal amount of CDGRCGVRY (*DGR-2C*) or CisoDGRCGVRY (*isoDGR-2C*). *C*, MALDI-TOF analysis of NGR-2C (expected monoisotopic mass, MH^+ 1025.43) at various time points during incubation (pH 8.5). The *arrows* indicate compounds corresponding to the succinimide intermediate.

To identify the degradation products corresponding to peaks 2 and 3, formed in ~1:3 ratio, we next analyzed heat-treated NGR-2C before and after spiking with NGR-2C or DGR-2C or *iso*DGR-2C. The results showed that peaks 2 and 3 correspond to DGR-2C and *iso*DGR-2C, respectively (Fig. 4*B*), suggesting that both degradation products are deamidated forms.

To verify this hypothesis and to assess whether the mechanism of deamidation occurs via succinimide intermediate we monitored the NGR-2C deamidation reaction by MALDI-TOF. This analytical method showed, as expected, a progressive decrease during incubation of the molecular species corresponding to NGR-2C (expected monoisotopic mass, MH^+ 1025.43) and an increase of species characterized by +1 Da (Fig. 4*C*). Noteworthy, a peak of −17 Da was also observed during the first 80 min of treatment, likely corresponding to the succinimide intermediate, which disappeared at later time points (Fig. 4*C*). These results strongly support the hypothesis that deamidation of Asn in the NGR motif occurs via loss of ammonia (−17 Da) followed by hydrolysis of the succinimide ring (+18 Da) with a global gain of ~1 Da, as has been demonstrated for other Asn-containing peptides (19–23).

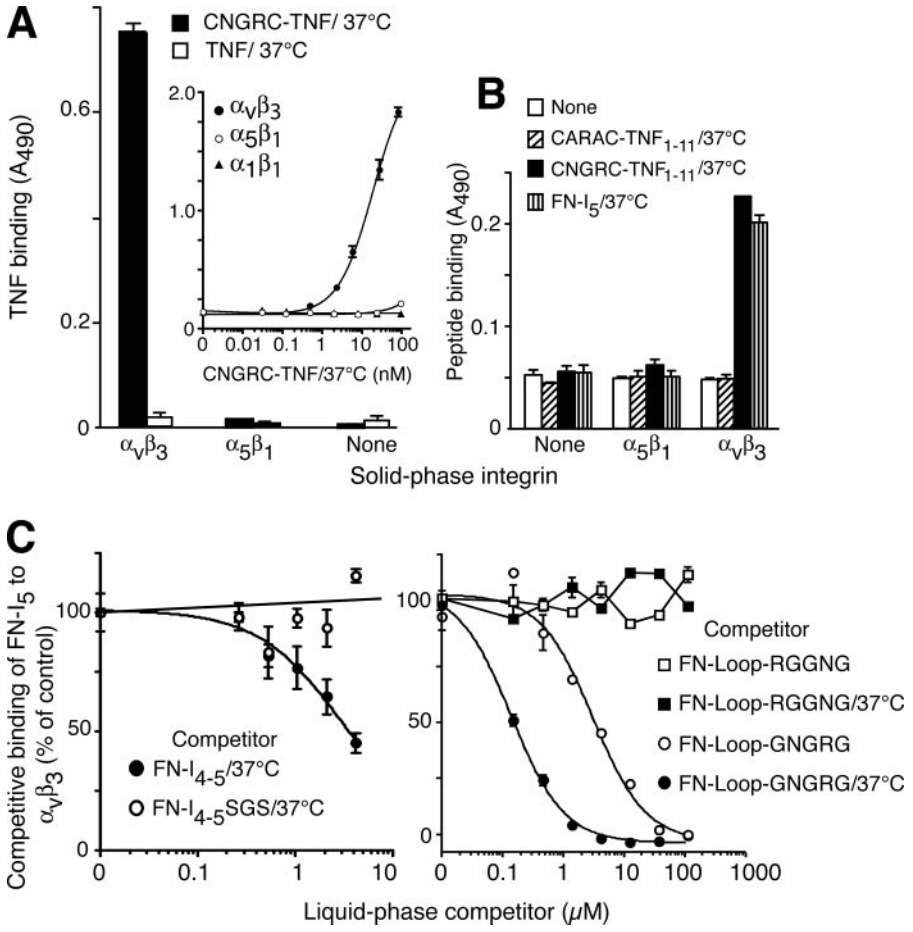

FIGURE 5. **FN-I_5 and peptides containing the NGR motif bind to $\alpha_v\beta_3$ integrin after accelerated aging.** *A*, binding of heat-treated CNGRC-TNF and TNF to solid phases coated with purified human integrins. Single concentration (5 μg/ml) or various concentrations (*inset*) of CNGRC-TNF and TNF were used. Binding was detected with anti-TNF antibodies as described under "Experimental Procedures." Mean ± S.E. (n = 2). *B*, binding of biotinylated CNGRC-TNF_{1-11}, CARAC-TNF_{1-11}, and FN-I_5 (complexed with streptavidin peroxidase) to purified human integrins. Binding was detected by chromogenic reaction with o-phenylendiamine. Mean ± S.E. (n = 2). *C*, competitive binding of biotinylated FN-I_5-streptavidin peroxidase complexes to $\alpha_v\beta_3$-coated plates with various amounts of FN-I_{4-5} or FN-I_{4-5}SGS (*left panel*) or peptides corresponding to the NGR loop (residues 258–271) of FN-I_5 before and after heat treatment (*right panel*). Mean ± S.E. (n = 4).

NGR. As expected, only the fragment with NGR competed the binding of FN-I_5 to $\alpha_v\beta_3$ (Fig. 5*C*, *left*). Binding competition was observed also with a peptide corresponding to the entire 256–271 loop of FN-I_5 (see Fig. 1*C*), but not with a control peptide with a scrambled sequence at the GNGRG site (Fig. 5, *right*). Similarly, the binding of CNGRC-TNF to $\alpha_v\beta_3$ was efficiently competed with heat-treated FN-I_5 (EC_{50}, 0.4 μM) (Fig. 6*A*).

To identify the NGR deamidation product responsible for integrin binding, other competitive ELISAs were performed using synthetic peptides with Asn replaced with Asp or *iso*Asp or Ser. The results showed that *iso*DGR-2C can compete 600-fold more efficiently than DGR-2C (EC_{50}, 0.1 *versus* 60 μM), whereas little or no competition occurred with the control peptide SGR-2C (EC_{50}, >1000 μM) (Fig. 6*A*). Furthermore, low efficiency was observed with D-*iso*DGR-2C, a peptide with D-*iso*Asp in place of L-*iso*Asp, indicating that the binding was stereospecific. Considering that the *iso*DGR-2C is stable under these assay conditions (see above), these results suggest that L-*iso*DGR is an $\alpha_v\beta_3$ binding motif.

Kinetics of Integrin Binding Site Formation in Fibronectin Fragments—To investigate the kinetics of integrin binding site formation in fibronectin fragments, we tested, by ELISA, the capability of FN-I_5 to compete the binding of CNGRC-TNF to $\alpha_v\beta_3$ after incubation for different times at 37 °C in DMEM. Interestingly, when we plotted the inhibitory concentrations (IC_{50}) *versus* incubation time we observed that maximal competitive binding activity was reached after 24–48 h of incubation (half-life 3.4 h) (Fig. 6*B*). This value corresponds very well to the time course of deamidation reaction of NGR-2C described above and further supports the concept that the integrin binding properties of heat-treated FN-I_5 were related to deamidation of the NGR site. Because the structural basis of heat-treated FN-I_5 function in cell adhesion is related to the presence of *iso*Asp we have named this product "isonectin-1" and we propose to call "isonectins" all bioactive fragments containing the deamidated FN-I_5 module.

L-isoDGR Is a Competitive Antagonist of RGD Ligands of $\alpha_v\beta_3$ and $\alpha_5\beta_1$ Integrins—To assess whether L-*iso*DGR binds the RGD binding site of $\alpha_v\beta_3$-integrin we next performed competitive binding studies with various doses of ACDCRGDCFC-TNF, a known high affinity ligand of $\alpha_v\beta_3$ integrin (15), and

$\alpha_v\beta_3$ Is a Receptor for the L-isoDGR Motif—In an attempt to identify the receptors of deamidated fibronectin fragments we analyzed the binding of heat-treated FN-I_5, as well as that of CNGRC-TNF and various peptides, to purified $\alpha_v\beta_3$, $\alpha_5\beta_1$, and $\alpha_1\beta_1$ integrins. To this aim, direct and competitive ELISAs with integrins adsorbed on microtiter plates were performed. Direct ELISA showed binding of all NGR-containing molecules (heat treated) to $\alpha_v\beta_3$ but little, or not at all, to the other integrins (Fig. 5, *A* and *B*). No binding was observed with heat-treated TNF or with a control CARAC-TNF_{1-11} peptide (Fig. 5, *A* and *B*), suggesting that NGR was critical. Of note, we observed binding of CNGRC-TNF to $\alpha_v\beta_3$ even before heat treatment, although to a lower extent (data not shown), possibly due to deamidation occurring during preparation and/or assay incubation. Accordingly, pretreatment with PIMT decreased the binding of both "heat-treated" and "untreated" CNGRC-TNF to $\alpha_v\beta_3$ (data not shown).

To verify the importance of the NGR loop of FN-I_5 for integrin binding we performed competitive binding experiments with recombinant FN-I_{4-5} and FN-I_{4-5}SGS, the latter lacking

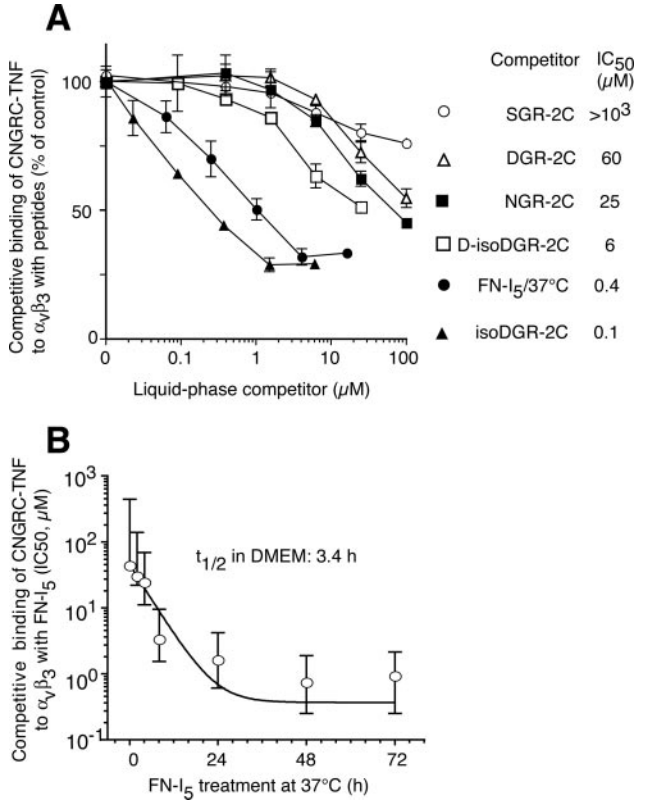

FIGURE 6. **Inhibition of CNGRC-TNF binding to $\alpha_v\beta_3$ by heat-treated FN-I_5 and by synthetic *iso*DGR-2C.** *A*, biotinylated CNGRC-TNF (4 μg/ml) was mixed with different amounts of the indicated peptides, added to $\alpha_v\beta_3$-coated plates, and left to incubate for 2 h at room temperature. Biotinylated CNGRC-TNF binding was detected with streptavidin peroxidase. Mean ± S.E. ($n = 2$). The concentration of each peptide able to compete 50% of binding (IC_{50}) is also shown. *B*, kinetics of FN-I_5 deamidation. FN-I_5 was diluted with DMEM and incubated for various times at 37 °C. The capability of each product to inhibit the binding of deamidated CNGRC-TNF to $\alpha_v\beta_3$ was then tested by competitive ELISA. The concentrations able to inhibit 50% of CNGRC-TNF binding (IC_{50}) obtained with each product were plotted *versus* the incubation times. *Bars* represent the confidence intervals.

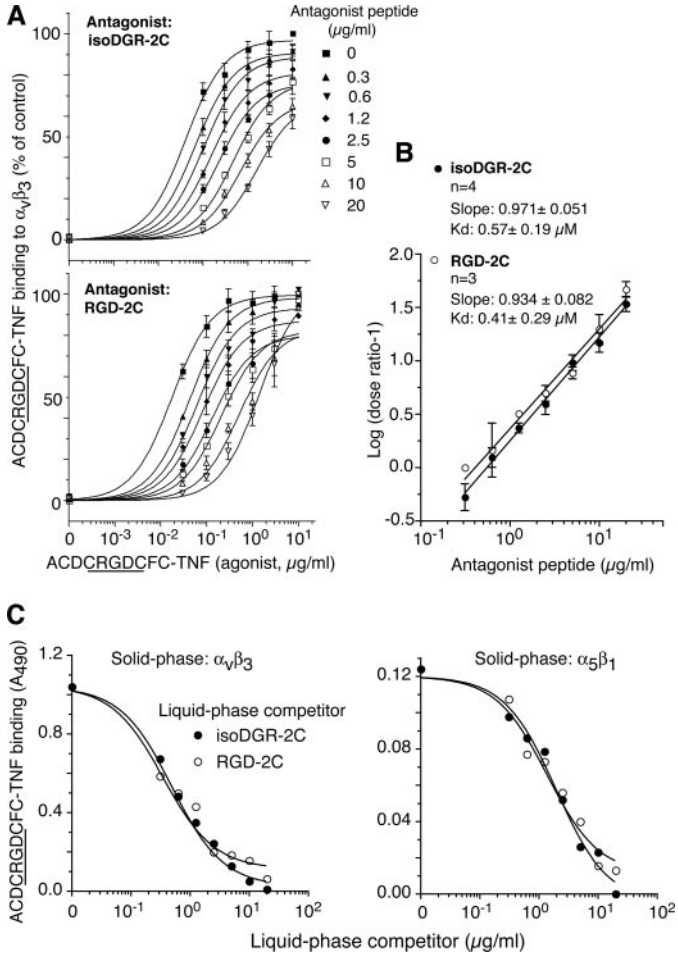

FIGURE 7. **L-*iso*DGR is a competitive antagonist of RGD ligands of $\alpha_v\beta_3$ and $\alpha_5\beta_1$ integrins.** *A*, competitive binding of ACDCRGDCFC-TNF to $\alpha_v\beta_3$ with CisoDGRCGVRY (*isoDGR-2C*) and CRGDCGVRY (*RGD-2C*). Microtiter plates were coated with $\alpha_v\beta_3$ and incubated with mixtures of ACDCRGDCFC-TNF (*agonist*) and peptides (*antagonists*) at the indicated concentrations. ACDCRGDCFC-TNF binding was detected with anti-TNF antibodies as described under "Experimental Procedures." *B,* Schild plot of binding data obtained using the Prism program (GraphPad Software, Inc., San Diego, CA). *C,* competitive binding of ACDCRGDCFC-TNF to $\alpha_v\beta_3$- or $\alpha_5\beta_1$-coated plates with the indicated peptides. In this case a single concentration of ACDCRGDCFC-TNF (0.1 μg/ml, *left panel;* 3 μg/ml, *right panel*) and various concentrations of competitor were used.

various doses of *iso*DGR-2C and RGD-2C (CRGDCGVRY). The binding curves and Schild plot of binding data showed that both peptides efficiently antagonize, in a competitive manner, the binding of ACDCRGDCFC-TNF to $\alpha_v\beta_3$-integrin (Fig. 7). This strongly suggests that the *iso*DGR motif binds within, or close to, the RGD binding site of $\alpha_v\beta_3$ with an affinity similar to that of the RGD motif (K_d 0.57 and 0.41 μM, respectively).

Because peptides containing CRGDC can also bind the $\alpha_5\beta_1$ integrin (32), we next performed competitive binding experiments with this integrin. As shown in Fig. 7*C*, the binding of ACDCRGDCFC-TNF to $\alpha_5\beta_1$ was weaker than that to $\alpha_v\beta_3$. The binding was competed by RGD-2C and *iso*DGR-2C with similar potency (Fig. 7*C*), suggesting that the *iso*DGR motif can also bind the RGD binding site of $\alpha_5\beta_1$. However, the IC_{50} was 4–5-fold higher than that required for $\alpha_v\beta_3$, suggesting that the affinity for this integrin was lower.

Deamidated FN-I_5 (Isonectin-1) Inhibits in Vitro Endothelial Cell Adhesion and Proliferation—Compounds able to inhibit the interaction of $\alpha_v\beta_3$ integrin, the vitronectin receptor, with ECM proteins are known to affect endothelial cell function and inhibit tumor growth (33–35). To assess whether isonectins can inhibit integrin-ECM protein interactions we have investigated the effect of soluble isonectin-1 on EA.hy926 endothelial cell adhesion to vitronectin-coated microtiter plates. These cells expressed CD31, $\alpha_v\beta_3$, $\alpha_v\beta_5$, β_4, β_1, α_6, and α_3 integrin subunits as checked by fluorescence-activated cell sorter analysis (data not shown). Isonectin-1 inhibited in a dose-dependent manner ~60% of cell adhesion to vitronectin (Fig. 8*A*), a protein that can interact with $\alpha_v\beta_3$, $\alpha_v\beta_5$, $\alpha_v\beta_1$, and $\alpha IIb\beta_3$ (36). Similarly, *iso*DGR-2C, but not SGR-2C, inhibited cell adhesion (Fig. 8*A*), strongly suggesting that *iso*DGR compounds may indeed work as antagonists of integrin-ECM interactions. Furthermore, both *iso*DGR-2C and RGD-2C, but not SGR-2C, inhibited the proliferation of human microvascular endothelial cells (HMEC-1) *in vitro* (Fig. 8*B*).

Isonectin-1 Inhibits Tumor Growth in Vivo—Because $\alpha_v\beta_3$-mediated endothelial cell adhesion is critical for endothelial cell survival and proliferation in tumors, we tested the hypothesis that isonectin-1 and *iso*DGR-2C peptide could affect tumor

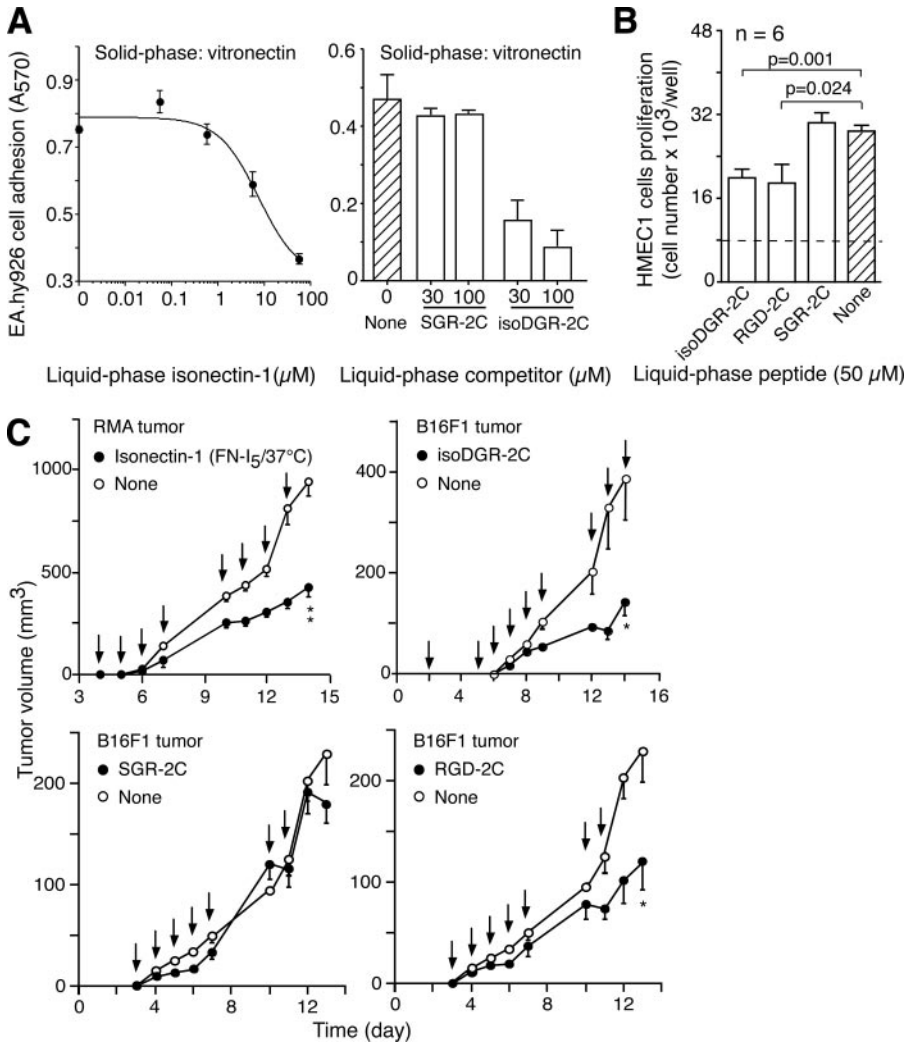

FIGURE 8. **Effect of deamidated FN-I_5 (*isonectin-1*), *iso*DGR-2C on endothelial cell adhesion, proliferation, and tumor growth.** *A*, inhibition of EA.hy926 cell adhesion to vitronectin by soluble isonectin-1 (prepared by heat treatment of FN-I_5), *iso*DGR-2C, and SGR-2C. Vitronectin (3 μg/ml) was adsorbed to microtiter plate, and cell adhesion assay was performed as described under "Experimental Procedures," using cell culture medium containing the soluble competitors. Mean ± S.E. ($n = 3$). *B*, inhibition of HMEC-1 cell proliferation by soluble *iso*DGR-2C, RGD-2C, and SGR-2C peptide. The assay was performed as described under "Experimental Procedures" using cell culture medium containing the soluble competitors. Mean ± S.E. ($n = 6$). *C*, anti-tumor effect of repeated administration of isonectin-1 (200 μg, intraperitoneal) to RMA tumor-bearing mice or *iso*DGR-2C or RGD-2C or SGR-2C peptide (100 μg, intraperitoneal) to B16F1 tumor-bearing mice as indicated. Animals (five/group) were treated at the indicated times (*arrows*). **, $p < 0.0005$; *, $p < 0.05$; statistical analysis by two-tailed *t* test.

growth. As expected, daily administration of isonectin-1 (200 μg, intraperitoneal) or *iso*DGR-2C (100 μg, intraperitoneal) to RMA lymphoma-or B16F1 melanoma-bearing mice, respectively, significantly inhibited tumor growth (Fig. 8*C*, *upper panels*). The effect was similar to that induced by RGD-2C peptide (Fig. 8*C*, *lower panel*), a known ligand of $\alpha_v\beta_3$ (32). Of note, the SGR-2C peptide, with *iso*Asp changed with Ser, was completely inactive, suggesting that the *iso*DGR motif was responsible for the observed anti-tumor activity.

DISCUSSION

It is well known that proteins may contain *iso*Asp residues due to post-translational Asn deamidation or Asp isomerization reactions (21, 31, 37–39). These reactions can occur *in vivo*, *e.g.* in extracellular matrix proteins with slow turnover (30, 31, 37), and *in vitro* during protein isolation and storage (22, 40, 41). In general these phenomena are associated with protein "loss of function" and, for this reason, are generally viewed as deleterious events associated with protein aging. In this work, for the first time we have shown that Asn deamidation of the NGR site of the fifth fibronectin type I repeat (FN-I_5) is associated with a gain of function, because deamidated fragments containing this module (named isonectins) are able to affect endothelial cell adhesion and proliferation in different assays.

This view is supported by the observation that (*a*) accelerated aging of synthetic FN-I_5 or recombinant FN-I_{4-5}, but not of FN-I_{4-5}-SGS (a mutant with the NGR sequence replaced with SGS), increased their cell adhesion properties; (*b*) accelerated aging was associated with Asn deamidation, as shown by mass spectrometry and *iso*Asp analysis of products; (*c*) treatment of aged fragments and peptides with PIMT, an enzyme that converts L-*iso*Asp and D-Asp residues to L-Asp (25, 27), completely inhibited their pro-adhesive activity.

We have obtained evidence to suggest that Asn deamidation at NGR sites occurs via succinimide intermediate, which upon hydrolytic cleavage leads to formation of Asp and *iso*Asp in a 1:3 ratio (see Fig. 9 for a schematic representation). Racemization and hydrolysis of the succinimide intermediate leading to the formation of D-Asp and D-*iso*Asp is also possible, but this typically occurs with a much lower efficiency (19, 20, 24). Thus, deamidated products with L-configuration are likely quantitatively more relevant. Deamidation reactions can take a few hours, days, or years to occur depending on neighboring amino acid sequence, temperature, buffer composition, and ionic strength (19, 21). For instance the presence of a Gly residue after Asn has a dramatic destabilizing effect (21, 22, 24). Accordingly, we have found that the kinetics of NGR deamidation in synthetic fibronectin fragments and peptides are surprisingly rapid (half-life 3–4 h), likely due to favorable conformation.

Three-dimensional structure analysis of FN-I_5 showed that the GNGRG motif forms an exposed loop, likely accessible to water and to receptors (see Fig. 1*B*). Of note, molecular dynamic simulation of an NGR peptide with flanking cysteines

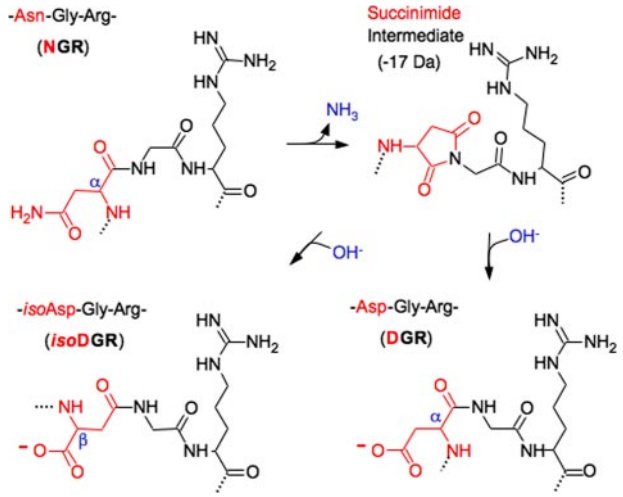

FIGURE 9. **Schematic representation of the NGR deamidation reaction.** Asparagine deamidation occurs via hydrolysis of the succinimide intermediate, leading to formation of DGR or *iso*DGR, with changes in charges and peptide bond length.

(CNGRC), used throughout this study as a molecular surrogate of the fibronectin NGR motif, showed that its structure is superimposable to that of the FN loop (8).

The question arises as to whether the receptor binding site in deamidated fibronectin is DGR or *iso*DGR. The following observations suggest that *iso*DGR is the biologically relevant motif. First, cell adhesion to deamidated FN-I_5 (named isonectin-1) was competed by peptides containing *iso*DGR but not the DGR motif. Noteworthy, no competition was observed with D-*iso*DGR-containing peptides, pointing to stereospecific interactions. Second, enzymatic conversion of L-*iso*Asp into L-Asp residues by PIMT completely inhibited the pro-adhesive activity of deamidated fibronectin fragments. This view is further supported by the observation that the CDGRC-TNF conjugate was completely inactive in direct cell adhesion assays. Thus, L-*iso*DGR is the bioactive motif.

Studies aimed at identifying the cellular binding sites showed that $\alpha_v\beta_3$ integrin efficiently binds deamidated FN-I_5 (isonectin-1) as well as peptides containing L-*iso*DGR, suggesting that this integrin is an important L-*iso*DGR receptor. A weaker binding was observed also with $\alpha_5\beta_1$. Noteworthy, D-*iso*DGR was 60-fold less efficient in $\alpha_v\beta_3$ binding. Furthermore, L-DGR was 600-fold less efficient in $\alpha_v\beta_3$ recognition, supporting the concept that L-*iso*DGR, and not L-DGR, is the bioactive motif. Furthermore, studies aimed at characterizing the binding site on $\alpha_v\beta_3$ and $\alpha_5\beta_1$ showed that L-*iso*DGR acts as a competitive inhibitor of the RGD binding site of these integrins.

Can Asn deamidation also occur in natural fibronectins? We have found that natural FN-30 kDa fragment as well as intact fibronectin freshly isolated from human plasma contain 0.026–0.048 pmol of *iso*Asp/pmol of protein. Furthermore, treatment of FN-30 kDa with PIMT partially inhibited its pro-adhesive properties. This suggests that formation of *iso*Asp can occur also in natural fibronectins in sufficient quantity to affect cell adhesion. We cannot exclude, however, that the kinetics of Asn deamidation in fibronectin might be slower than that measured with peptides or with FN-I_5, considering the strong influence that the Asn molecular microenvironment might have on deamidation kinetics. One interesting possibility that deserves to be investigated is that conformational changes occurring after deposition in tissues or local changes in the microenvironment composition or the presence of specific proteases might affect the kinetics of this reaction. Considering the low turnover of fibronectin after deposition in tissues (42) and the abundance of this protein in plasma and in tissues, it is very likely that a significant amount of deamidated fibronectin is formed also *in vivo*. Another question is whether generation/removal of *iso*DGR in fibronectin could play a role in normal or pathological conditions. We observed that isonectin-1 can inhibit the adhesion of endothelial cells to vitronectin, a ligand of $\alpha_v\beta_3$; furthermore, peptides containing the *iso*DGR motif inhibited the proliferation of microvascular endothelial cells *in vitro*. We have also observed that daily administration of isonectin-1 to RMA lymphoma-bearing mice significantly inhibits tumor growth *in vivo*. These findings suggest that deamidated fragments may play a role in endothelial cell adhesion and tumor biology. Several investigators implicated $\alpha_v\beta_3$ as a receptor for various proteolytic fragments of ECM proteins that can act as anti-angiogenic factors (43–45). An interesting possibility is that deamidated fibronectin fragments contribute, together with other ECM protein fragments, to regulate angiogenesis in normal and pathological conditions.

How can cells control *iso*DGR generation in fibronectin? Asn deamidation is a thermodynamically spontaneous reaction independent from enzymatic regulation. Whether specific deamidases further accelerating this process exist or not is presently unknown. However, the finding that enzymatic removal of *iso*Asp by PIMT inhibits isonectin-1 pro-adhesive activity suggests a potential enzymatic mechanism for negative regulation of this site. Formation of β-linked isopeptide bond (*iso*Asp) in proteins and subsequent conversion in α-linked peptide bond (Asp) by PIMT are generally regarded as a sort of "damage repair" mechanism of aged proteins (31). It has also been hypothesized that in some proteins these damage repair reactions may have some useful function, *e.g.* as a sort of molecular clock for protein degradation or intracellular localization (21, 31, 46). Based on our findings, a new "activation-deactivation" model may also be envisaged for *iso*Asp formation-removal occurring at certain sites in extracellular proteins (selected by evolution), such as fibronectin. Thus, whereas PIMT may be considered a sort of "repairing" enzyme for Asp residues undergoing isomerization, *e.g.* to rescue RGD in aged fibronectin and collagen (30, 31), it may also be viewed as an enzyme that "destroys" the function of *iso*DGR, pointing to a new function for this enzyme. Of note, increased amounts of extracellular PIMT have been observed in injured tissues and wound healing (47, 48).

Finally, considering that $\alpha_v\beta_3$ integrin is a good marker of angiogenic vessels, exogenous fibronectin fragments or short peptides containing the L-*iso*DGR motif may be exploited, in principle, as ligand for targeted delivery of drugs, cytokines, toxins, apoptotic peptides, radionuclides, viral particles, genes, or imaging compounds to angiogenic vessels in tumors or in other angiogenesis-related diseases.

In conclusion, spontaneous conversion of NGR to *iso*DGR in fibronectin fragments represents a novel mechanism for gener-

ating $\alpha_v\beta_3$ ligands that may regulate endothelial cell functions and tumor growth. Generation of *iso*DGR sites in proteins by NGR deamidation (or DGR isomerization) may represent a novel mechanism for regulating their function.

Acknowledgments—We thank Angelina Sacchi and Barbara Colombo for technical assistance in in vivo experiments.

REFERENCES

1. Pankov, R., and Yamada, K. M. (2002) *J. Cell Sci.* **115,** 3861–3863
2. Humphries, M. J., Obara, M., Olden, K., and Yamada, K. M. (1989) *Cancer Investig.* **7,** 373–393
3. Mohri, H. (1997) *Peptides* **18,** 899–907
4. Yamada, K. M. (1989) *Curr. Opin. Cell Biol.* **1,** 956–963
5. Plow, E. F., Haas, T. A., Zhang, L., Loftus, J., and Smith, J. W. (2000) *J. Biol. Chem.* **275,** 21785–21788
6. Johansson, S., Svineng, G., Wennerberg, K., Armulik, A., and Lohikangas, L. (1997) *Front. Biosci.* **2,** d126–146
7. Pytela, R., Pierschbacher, M. D., and Ruoslahti, E. (1985) *Cell* **40,** 191–198
8. Di Matteo, P., Curnis, F., Longhi, R., Colombo, G., Sacchi, A., Crippa, L., Protti, M. P., Ponzoni, M., Toma, S., and Corti, A. (2006) *Mol. Immunol.* **43,** 1509–1518
9. Koivunen, E., Gay, D. A., and Ruoslahti, E. (1993) *J. Biol. Chem.* **268,** 20205–20210
10. Ljunggren, H. G., and Karre, K. (1985) *J. Exp. Med.* **162,** 1745–1759
11. Curnis, F., Gasparri, A., Sacchi, A., Cattaneo, A., Magni, F., and Corti, A. (2005) *Cancer Res.* **65,** 2906–2913
12. Akiyama, S. K., and Yamada, K. M. (1995) in *Extracellular Matrix: A Practical Approach* (Haralson, M. A., and Hassel, J. R., eds) pp. 175–185, Oxford University Press, New York
13. Tanzarella, S., Russo, V., Lionello, I., Dalerba, P., Rigatti, D., Bordignon, C., and Traversari, C. (1999) *Cancer Res.* **59,** 2668–2674
14. Curnis, F., Sacchi, A., Borgna, L., Magni, F., Gasparri, A., and Corti, A. (2000) *Nat. Biotechnol.* **18,** 1185–1190
15. Curnis, F., Gasparri, A., Sacchi, A., Longhi, R., and Corti, A. (2004) *Cancer Res.* **64,** 565–571
16. Colombo, G., Curnis, F., De Mori, G. M., Gasparri, A., Longoni, C., Sacchi, A., Longhi, R., and Corti, A. (2002) *J. Biol. Chem.* **277,** 47891–47897
17. Corti, A., Poiesi, C., Merli, S., and Cassani, G. (1994) *J. Immunol. Meth.* **177,** 191–198
18. Gasparri, A., Moro, M., Curnis, F., Sacchi, A., Pagano, S., Veglia, F., Casorati, G., Siccardi, A. G., Dellabona, P., and Corti, A. (1999) *Cancer Res.* **59,** 2917–2923
19. Tyler-Cross, R., and Schirch, V. (1991) *J. Biol. Chem.* **266,** 22549–22556
20. Stephenson, R. C., and Clarke, S. (1989) *J. Biol. Chem.* **264,** 6164–6170
21. Robinson, N. E., and Robinson, A. B. (2001) *Proc. Natl. Acad. Sci. U. S. A.* **98,** 944–949
22. Robinson, N. E., Robinson, Z. W., Robinson, B. R., Robinson, A. L., Robinson, J. A., Robinson, M. L., and Robinson, A. B. (2004) *J. Pept. Res.* **63,** 426–436
23. Fuzery, A. K., Mihala, N., Szabo, P., Perczel, A., Giavazzi, R., and Suli-Vargha, H. (2005) *J. Pept. Sci.* **11,** 53–59
24. Geiger, T., and Clarke, S. (1987) *J. Biol. Chem.* **262,** 785–794
25. McFadden, P. N., and Clarke, S. (1987) *Proc. Natl. Acad. Sci. U. S. A.* **84,** 2595–2599
26. Galletti, P., Ingrosso, D., Manna, C., Sica, F., Capasso, S., Pucci, P., and Marino, G. (1988) *Eur. J. Biochem.* **177,** 233–239
27. Lowenson, J. D., and Clarke, S. (1992) *J. Biol. Chem.* **267,** 5985–5995
28. Aswad, D. W. (1984) *J. Biol. Chem.* **259,** 10714–10721
29. Murray, E. D., Jr., and Clarke, S. (1984) *J. Biol. Chem.* **259,** 10722–10732
30. Lanthier, J., and Desrosiers, R. R. (2004) *Exp. Cell Res.* **293,** 96–105
31. Reissner, K. J., and Aswad, D. W. (2003) *Cell. Mol. Life Sci.* **60,** 1281–1295
32. Koivunen, E., Wang, B., and Ruoslahti, E. (1995) *Bio/Technology* **13,** 265–270
33. Hynes, R. O. (2002) *Nat. Med.* **8,** 918–921
34. Brooks, P. C., Montgomery, A. M., Rosenfeld, M., Reisfeld, R. A., Hu, T., Klier, G., and Cheresh, D. A. (1994) *Cell* **79,** 1157–1164
35. Hammes, H. P., Brownlee, M., Jonczyk, A., Sutter, A., and Preissner, K. T. (1996) *Nat. Med.* **2,** 529–533
36. Felding-Habermann, B., and Cheresh, D. A. (1993) *Curr. Opin. Cell Biol.* **5,** 864–868
37. Lindner, H., and Helliger, W. (2001) *Exp. Gerontol.* **36,** 1551–1563
38. Robinson, N. E. (2002) *Proc. Natl. Acad. Sci. U. S. A.* **99,** 5283–5288
39. Robinson, A. B., McKerrow, J. H., and Cary, P. (1970) *Proc. Natl. Acad. Sci. U. S. A.* **66,** 753–757
40. Paranandi, M. V., Guzzetta, A. W., Hancock, W. S., and Aswad, D. W. (1994) *J. Biol. Chem.* **269,** 243–253
41. Najbauer, J., Orpiszewski, J., and Aswad, D. W. (1996) *Biochemistry* **35,** 5183–5190
42. Pussell, B. A., Peake, P. W., Brown, M. A., and Charlesworth, J. A. (1985) *J. Clin. Investig.* **76,** 143–148
43. Brooks, P. C., Silletti, S., von Schalscha, T. L., Friedlander, M., and Cheresh, D. A. (1998) *Cell* **92,** 391–400
44. Tarui, T., Miles, L. A., and Takada, Y. (2001) *J. Biol. Chem.* **276,** 39562–39568
45. Rehn, M., Veikkola, T., Kukk-Valdre, E., Nakamura, H., Ilmonen, M., Lombardo, C., Pihlajaniemi, T., Alitalo, K., and Vuori, K. (2001) *Proc. Natl. Acad. Sci. U. S. A.* **98,** 1024–1029
46. Pepperkok, R., Hotz-Wagenblatt, A., Konig, N., Girod, A., Bossemeyer, D., and Kinzel, V. (2000) *J. Cell Biol.* **148,** 715–726
47. Weber, D. J., and McFadden, P. N. (1997) *J. Protein Chem.* **16,** 257–267
48. Weber, D. J., and McFadden, P. N. (1997) *J. Protein Chem.* **16,** 269–281

Spontaneous Formation of L-Isoaspartate and Gain of Function in Fibronectin

Flavio Curnis, Renato Longhi, Luca Crippa, Angela Cattaneo, Eleonora Dondossola, Angela Bachi and Angelo Corti

J. Biol. Chem. 2006, 281:36466-36476.
doi: 10.1074/jbc.M604812200 originally published online October 2, 2006
